Effect of an in-plane magnetic field on the spin transport through a Rashba superlattice

Ya Zhang* and Feng Zhai†
School of Physics and Optoelectronic Technology, College of Advanced Science and Technology, Dalian University of Technology, Dalian 116024, China

(Received 25 July 2008; revised manuscript received 4 December 2008; published 17 February 2009)

We investigate spin-dependent transport properties of a single-channel planar electron waveguide under a periodic modulation of Rashba spin-orbit interaction (SOI) and subject to a weak in-plane magnetic field $\mathbf{B}_{\text{in}}$. The spatially periodic variation in the Rashba SOI strength gives rise to a band structure with full band gaps. The inclusion of $\mathbf{B}_{\text{in}}$ with a proper orientation angle θ (relative to the transport direction) introduces local band gaps where only two propagating (one right going and one left going) modes exist. As a result, for a finite superlattice with a sufficient number of periodic units, the generated spin polarization and its direction depend strongly on θ. For a given Fermi energy higher than the Zeeman potential, there may exist several intervals of θ within which an optimal spin polarization is achieved.

DOI: 10.1103/PhysRevB.79.085311 PACS number(s): 72.25.Dc, 71.70.Ej, 85.75.−d, 73.23.Ad

I. INTRODUCTION

In recent years there has been a great deal of research interest on the interaction between the spin and the orbital degrees of freedom of carriers in semiconductors.[1] The reason is that the spin-orbit interaction (SOI) offers an electric pathway to manipulate the electron spin, which lies at the heart of spintronics. In semiconductors the presence of a strong structural or crystal inversion asymmetry gives rise to the so-called Rashba[2] or Dresselhaus[3] SOI. The Rashba SOI can be tuned by one or several voltage gates.[4–7] The SOI has been utilized to devise various spintronic devices such as spin transistors,[8,9] spin logic,[10,11] and spin filters.[12–16]

As for spin filtering properties of two-terminal quantum wire systems, the SOI alone cannot generate a spin-polarized transmitted electron beam when the output lead supports only one orbital channel.[17] This fact arises from the time-reversal symmetry. It has been shown theoretically that a remarkable spin polarization can be achieved when the time-reversal symmetry is broken by the inclusion of a proper weak magnetic field[18,19] in those SOI systems. In Ref. 19 a spin filter has been put forward based on a one-dimensional (1D) semiconductor quantum wire modulated by both a periodic Rashba SOI and a uniform in-plane magnetic field $\mathbf{B}_{\text{in}}$. In their studies, the direction of $\mathbf{B}_{\text{in}}$ is fixed to be perpendicular to the wire axis. Two separated superlattice energy gaps for spin-up and spin-down electrons result in a nearly complete spin polarization within two energy intervals. Note that for such a kind of system the angle of $\mathbf{B}_{\text{in}}$ with respect to the one-dimensional conducting channel, θ, can significantly modify the band structure. For example, for a uniform Rashba wire a pseudogap is present as long as $\theta \neq \pm \pi/2$ and has a maximal width when $\mathbf{B}_{\text{in}}$ is in parallel to the wire axis.[20,21] Thus an interesting question arises: how does the magnetic field direction affect the dispersive relation and spin polarization of a Rashba superlattice? In this work we examine this problem to find the angle θ under which the electron spin is polarized most effectively.

II. MODEL AND FORMALISM

The system we consider is a two-dimensional electron gas (2DEG) in the (x,z) plane contained in an asymmetric quantum well. The SOI therein is assumed to arise dominantly from the linear Rashba mechanism,

$$H_{\text{SO}} = [\alpha(\sigma_x p_z - \sigma_z p_x) + \text{H.c.}]/2\hbar. \tag{1}$$

Here σ_x, σ_y, and σ_z are three Pauli matrices and α represents the strength of the Rashba SOI. A hard-wall confining potential is further applied to the 2DEG to form a quantum waveguide along the x direction. We limit our attention to the situation where the waveguide width is much smaller than the electron Fermi wavelength so that the device can be treated as a 1D quantum wire. By the application of a series of voltage gates[6] a periodic SOI modulation can be achieved, as sketched in Fig. 1. For simplicity, we take a piecewise distribution of the SOI strength, that is, α takes alternatively 0 and a constant value α_0 in adjacent regions (see Fig. 1). Note that a smooth distribution of SOI strength gives rise to similar results. All regions have the same length $a/2$ with a the periodic length. An in-plane magnetic field $\mathbf{B}_{\text{in}}$ is applied with a tilted angle θ with respect to the transport x direction. The waveguide is connected with two nonmagnetic leads with a vanishing SOI and magnetic field.

The considered system can be described by the following single-particle Hamiltonian:

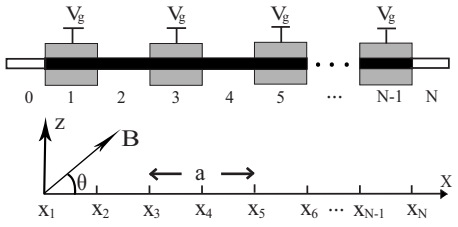

FIG. 1. Schematic illustration of the considered single-channel waveguide structure within the (x,z) plane. A series of voltage gates are applied to form a periodic Rashba SOI modulation. Both the SOI regions and non-SOI regions have the same length $a/2$ with a the superlattice period. An in-plane magnetic field is applied with a titled angle θ relative to the transport x direction.

$$H = \frac{p_x^2}{2m^*} + V_0(\sigma_z \sin\theta + \sigma_x \cos\theta) + H_{\mathrm{SO}}, \tag{2}$$

where m^* is the effective mass of electrons and V_0 indicates the Zeeman energy associated with $\mathbf{B}_{\mathrm{in}}$. Note that the electron spin along the transverse z direction is conserved only for the case of $\theta = \pm\pi/2$ which is considered in Ref. 19. We take the z direction as the spin-quantization axis. The vector potential caused by the magnetic field $\mathbf{B}_{\mathrm{in}}$ can be safely neglected in the weak-field limit where the magnetic length is much larger than the width of the confining well.

In a region with a constant SOI strength α and for a given energy E, the eigenwavefunctions of Eq. (2) can be written as

$$\Psi_k = e^{ikx}\begin{pmatrix} a_k \\ b_k \end{pmatrix}, \tag{3}$$

where the wave vector k and the spinor are determined from

$$\begin{pmatrix} \frac{\hbar^2k^2}{2m^*} + V_0\sin\theta - \alpha k - E & V_0\cos\theta \\ V_0\cos\theta & \frac{\hbar^2k^2}{2m^*} - V_0\sin\theta + \alpha k - E \end{pmatrix} \times \begin{pmatrix} a_k \\ b_k \end{pmatrix} = 0. \tag{4}$$

Equation (4) leads to a nonlinear equation of k. We can map it onto an equivalent eigenvalue problem as in Ref. 22 to obtain its four solutions and the corresponding eigenvectors. A real solution of k gives a propagating mode, whose propagating direction ("forward or backward") can be identified from the sign (+/−) of its average velocity, v_k. The expression of v_k is given by

$$v_k = \Psi_k^+\left(\frac{p_x}{m^*} - \frac{\alpha}{\hbar}\sigma_z\right)\Psi_k. \tag{5}$$

A complex solution of k indicates either an evanescent (Im $k>0$) or an exploding (Im $k<0$) mode from the view of the forward direction.

For an electron incident from the left lead with spin $\sigma_L(=\uparrow\downarrow)$ and energy E, the transmitted wave function in the right lead consists of both spin-conserved and spin-flipped components generally,

$$\Psi^R_{\sigma_L}(x) = e^{ik_Rx}(t_{\uparrow_{\sigma_L}}|\uparrow\rangle + t_{\downarrow_{\sigma_L}}|\downarrow\rangle), \tag{6}$$

where $t_{\uparrow_{\sigma_L}}$ and $t_{\downarrow_{\sigma_L}}$ are the transmission amplitudes and $k_R = \sqrt{2m^*E}/\hbar$. Note that k_R is spin independent due to the assumption of a vanishing magnetic field and SOI in leads. The scattering matrix method[23] is adopted to evaluate those transmission amplitudes, which is numerically stable even for strongly modulated systems. Note that the transfer-matrix method (which was used in Ref. 19) may not be reliable numerically when $E<V_0$ due to the appearance of both fast growing and fast decaying exponential terms in the transfer matrix.[23] The spin-dependent conductances are

$$G_{\sigma_R\sigma_L} = G_0|t_{\sigma_R\sigma_L}|^2 \tag{7}$$

with $G_0=e^2/h$ and $\sigma_R=\uparrow\downarrow$. For the considered case of spin-unpolarized injection, the spin polarization of transmitted electron beam can be calculated as[17]

$$P_x + iP_y = \frac{2G_0}{G}\sum_{\sigma_L} t_{\downarrow\sigma_L}t^*_{\uparrow\sigma_L}, \tag{8}$$

$$P_z = \frac{(G_{\uparrow\uparrow}+G_{\uparrow\downarrow}) - (G_{\downarrow\downarrow}+G_{\downarrow\uparrow})}{G}, \tag{9}$$

where the total conductance is $G=G_{\uparrow\uparrow}+G_{\uparrow\downarrow}+G_{\downarrow\downarrow}+G_{\downarrow\uparrow}$.

In what follows the electron effective mass is taken to be $0.04m_0$ (m_0 is the free-electron mass), which is appropriate to an InGaAs quantum well system.[7] The Rashba strength in the SOI regions is set at $\alpha_0=30$ meV nm, a realistic value for 2DEGs fabricated from $In_{0.75}Ga_{0.25}As/In_{0.75}Al_{0.25}As$ heterostructures.[24] The superlattice period is fixed at $a=60$ nm.

III. BAND STRUCTURES OF AN IDEAL RASHBA SUPERLATTICE

In order to understand the effect of the magnetic field direction on the spin polarization of the considered system, it is instructive to begin with the electron energy band structures of an ideal Rashba superlattice. The band structures can be calculated numerically by the expansion of the Bloch wave functions Φ_k in plane waves $\Phi_{m\sigma;k}(x)=\exp[i(k+2m\pi/a)x]|\sigma\rangle/\sqrt{a}$, i.e.,

$$\Phi_k = \sum_{m=-\infty}^{\infty}\sum_{\sigma=\pm1} c_{m\sigma}(k)\Phi_{m\sigma;k}. \tag{10}$$

The eigenenergy $E(k)$ and the coefficients $c_{m\sigma}(k)$ are obtained from the eigenequation

$$\sum_{m\sigma}\left[\int_0^a dx\Phi^+_{m'\sigma';k}(x)H\Phi_{m\sigma;k}(x) - E(k)\delta_{mm'}\delta_{\sigma\sigma'}\right] \times c_{m\sigma}(k) = 0. \tag{11}$$

For the special case $\theta=\pi/2$ an analytical expression for $E(k)$ can be derived by the help of a local unitary transformation, $\Phi_k(x)=U(x)\Phi'_k(x)$,

$$U(x) = \exp\left[i\sigma_z\frac{m^*}{\hbar^2}\int_0^x \alpha(x')dx'\right]. \tag{12}$$

The continuity condition for Φ_k is equivalent to that Φ'_k and its derivative are continuous everywhere, while the periodic boundary condition $\Phi_k(x+a)=\exp(ika)\Phi_k(x)$ is translated into $\Phi'_k(x+a)=\exp(ika)U(-a)\Phi'_k(x)$. Note that Hamiltonian (2) (for $\theta=\pi/2$) is transformed into

$$H' = U^{-1}(x)HU(x) = \frac{p_x^2}{2m^*} - \frac{m^*\alpha^2(x)}{2\hbar^2} + V_0\sigma_z. \tag{13}$$

In the nth SOI region $\Phi'_k(x)$ can be expressed as $a_n\exp[ik_1(x-na)]+b_n\exp[-ik_1(x-na)]$ with

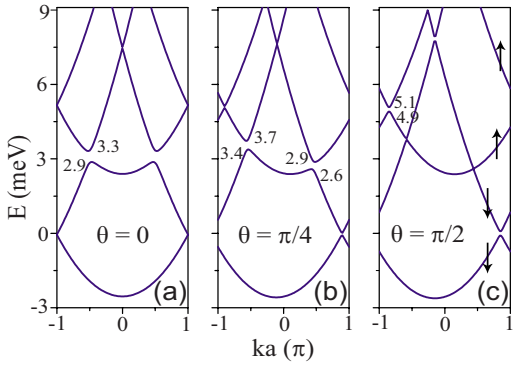

FIG. 2. (Color online) The lowest four energy bands of an ideal Rashba superlattice with a periodic length $a=60$ nm modulated by an in-plane magnetic field. Three values of the magnetic field orientation angle θ are considered: (a) 0, (b) $\pi/4$, and (c) $\pi/2$. The data given in each panel represent the energy interval of corresponding band gap. The arrows in (c) indicate the spin orientation of subbands. The Zeeman potential is set at $V_0=2.5$ meV and the Rashba strength in each SOI region is $\alpha_0=30$ meV nm.

$$k_1 = \sqrt{2m^*(E - V_0\sigma)/\hbar^2 + (\alpha_0 m^*/\hbar^2)^2}. \tag{14}$$

The expansion coefficients of adjacent units are connected by a 2×2 transfer matrix M, i.e., $(a_{n+1},b_{n+1})^T = M(a_n,b_n)^T$. Note that when we introduce another wave vector

$$k_2 = \sqrt{2m^*(E - V_0\sigma)/\hbar^2}, \tag{15}$$

the form of M is the same as that in the Kronig-Penny model, while the dispersion relation is determined by $\mathrm{tr}\, M = 2\cos(ka - \sigma\Theta)$ with $\Theta = \int_0^a \alpha(x)(m^*/\hbar^2)dx = (a/2)m^*\alpha_0/\hbar^2$. The transcendental equation is given by

$$\cos(ka - \sigma\Theta) = \cos\frac{k_1 a}{2}\cos\frac{k_2 a}{2} - \frac{k_1^2 + k_2^2}{2k_1 k_2}\sin\frac{k_1 a}{2}\sin\frac{k_2 a}{2}. \tag{16}$$

In Fig. 2 we plot the lowest four energy bands for three field angles ($\theta=0$, $\pi/4$, and $\pi/2$) as functions of the Bloch wave vector $k \in [-\pi/a, \pi/a]$. The Zeeman energy is taken to be $V_0=2.5$ meV. In all cases, energy gaps appear due to the periodic variation in the SOI strength.[25] Distinct band-gap features for the three field angles can also be observed from the figure. When $\mathbf{B}_{\mathrm{in}}$ is in parallel with the wire axis ($\theta=0$), the band curves are symmetric with respect to the central wave vector $k=0$. This is guaranteed by the symmetry associated with the operation $\sigma_x R_x$, where R_x is the reflection operator $x \to 2x_c - x$ (x_c is a central point of the superlattice). The operation $\sigma_x R_x$ transforms a Bloch state $\exp(ikx)u(x)$ [$u(x+a)=u(x)$ is a spinor] with wave vector k to a Bloch state $\exp(-ikx)[\sigma_x u(x)]$ with wave vector $-k$.[17] A full energy gap opens from 2.9 meV to 3.3 meV. When $\mathbf{B}_{\mathrm{in}}$ is perpendicular to the transport channel ($\theta=\pi/2$), the z component of electron spin is conserved and can be used to label the bands. The bands are strongly asymmetric relative to $k=0$. From Fig. 2(c) one can see that the gap intervals of the spin-up subbands and those of spin-down subbands have no overlap for the considered V_0. This is crucial for the spin filtering scheme proposed in Ref. 19. It can be seen from Eq. (16) that

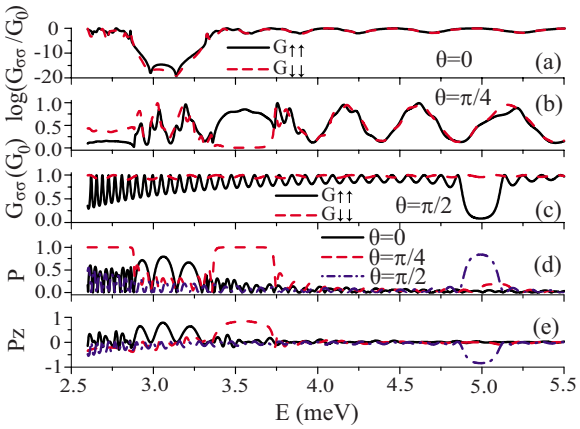

FIG. 3. (Color online) Spin-dependent conductances and spin polarization of a Rashba superlattice plotted as functions of the incident energy for three angles of $\mathbf{B}_{\mathrm{in}}$ ($\theta=0$, $\pi/4$, and $\pi/2$). [(a)–(c)] Spin-conserved conductances $G_{\uparrow\uparrow}$ and $G_{\downarrow\downarrow}$; (d) total spin polarization P; (e) spin-polarization projection along the z axis, P_z. The Zeeman potential is $V_0=2.5$ meV. The number of periodic units of the Rashba superlattice is 50. Note that in (a) the normalized conductances are plotted in a 10-based logarithmic scale.

the extremum point k_σ for the σ spin subbands satisfies

$$k_\sigma a = \sigma\Theta + m\pi \in [-\pi, \pi], \tag{17}$$

where m is integer. Thus $k_+ = -k_-$, as seen in Fig. 2(c). For the middle case $\theta=\pi/4$, no full band gap appears as in the situation $\theta=\pi/2$. However, there are several local energy gaps, such as [2.6, 2.9] and [3.4, 3.7] meV, in which only two propagating (one right going and one left going) modes exist. These local band gaps are crucial for the appearance of nearly complete spin polarization in a finite Rashba superlattice (with a sufficient number of periodic units).

IV. SPIN TRANSPORT OF A FINITE RASHBA SUPERLATTICE

Figure 3 presents the spin-dependent conductances and spin polarizations as functions of the Fermi energy, for three magnetic field orientations considered in Fig. 2. The number of periodic units of the finite Rashba superlattice is chosen to be 50 and the Zeeman potential is still set at $V_0=2.5$ meV. For all magnetic field angle θ the two spin-flipped conductances, $G_{\uparrow\downarrow}$ and $G_{\downarrow\uparrow}$ (not shown in Fig. 3), coincide because the system Hamiltonian is invariant under the operation $\sigma_y R_x T$, where T is the time-reversal operator.[17] Thus the polarization component P_z is contributed by the difference of the two spin-conserved conductances, $G_{\uparrow\uparrow}$ and $G_{\downarrow\downarrow}$. For $\theta=0$ we observe a slight relative difference between them in Fig. 3(a), except within the energy region [2.9, 3.3] meV, which is a full band gap of the corresponding ideal superlattice [see Fig. 2(a)]. The conductance is usually rather small when the Fermi energy falls into such a gap, as exhibited in Fig. 3(a). The spin polarization within this energy interval is remarkable [see Figs. 3(d) and 3(e)], as a result of spin-dependent tunneling. For $\theta=\pi/2$, we have $G_{\uparrow\downarrow}=G_{\downarrow\uparrow}=0$ and $P_x=P_y=0$. The $G_{\uparrow\uparrow}$ curve plotted in Fig. 3(c) exhibits a rapid

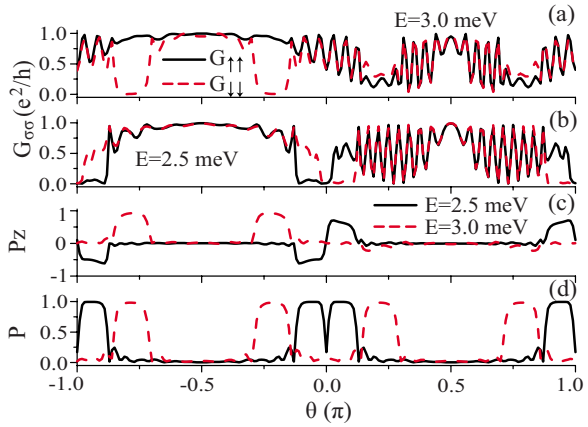

FIG. 4. (Color online) Spin-dependent conductances and spin polarization of a Rashba superlattice plotted as functions of the magnetic field angle θ for two Fermi energies, $E=3$ and 2.5 meV. [(a)–(b)] Spin-conserved conductances $G_{\uparrow\uparrow}$ and $G_{\downarrow\downarrow}$; (c) spin-polarization projection along the z axis, P_z; (d) total spin polarization P. The Zeeman potential is $V_0=1$ meV. The number of periodic units of the Rashba superlattice is 50.

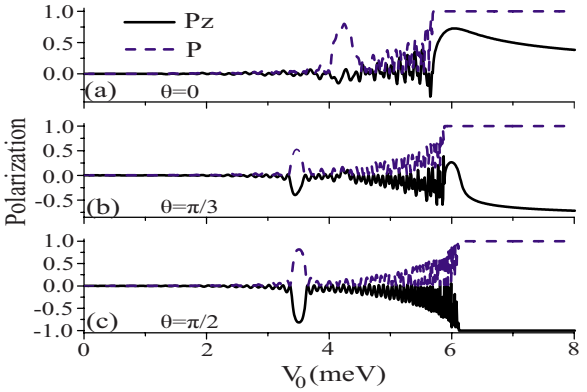

FIG. 5. (Color online) Spin-polarization component P_z and total polarization P of a Rashba superlattice plotted as functions of the Zeeman potential V_0 for three magnetic field angles (a) 0, (b) $\pi/3$, and (c) $\pi/2$. The Fermi energy is $E=6$ meV. The number of periodic units of the Rashba superlattice is 50.

oscillation with the Fermi energy and a valley in the energy interval [4.9, 5.1] meV, which lies in a spin-up subband gap [see Fig. 2(c)]. $G_{\downarrow\downarrow}$ shows a slight variation around the value e^2/h within the whole considered energy region (its valley is centered at 20.9 meV and is shallow). Thus we observe only a single polarization valley in Fig. 3(e), which differs from the results in Ref. 19 where two wide plateaus of P_z with values ± 1 are obtained. For $\theta=\pi/4$, the polarization curve plotted in Fig. 3(d) demonstrates two wide plateaus with a value nearly 100%. The positions of the plateaus are also in agreement with the band structures shown in Fig. 2(b). In comparison with Fig. 3(e) we know that the spin-polarization vector has a large in-plane component within the two plateaus. A full polarization means electrons with spin opposite to the polarization direction are almost totally reflected.[18] This is partly indicated in Fig. 3(b).

The results shown in Fig. 3 imply that a proper magnetic field orientation can enhance the spin polarization of the considered system. This is reflected more clearly in Fig. 4 where the spin-conserved conductances and the spin polarizations are plotted as functions of the magnetic field angle θ for two Fermi energy values ($E=3$ and 2.5 meV). We set the Zeeman potential at 1 meV. It can be seen that both $G_{\uparrow\uparrow}$ and $G_{\downarrow\downarrow}$ are symmetric relative to the line $\theta=\pm\pi/2$, that is, $G_{\sigma\sigma}(\pi-\theta)=G_{\sigma\sigma}(\theta)$. The reason is that the operation σ_z is equivalent to changing the magnetic field orientation from θ to $\pi-\theta$. The symmetry analysis gives rise to

$$P_{x,y}(\pi-\theta)=-P_{x,y}(\theta), \quad P_z(\pi-\theta)=P_z(\theta). \tag{18}$$

These restrictions imposed on the spin polarization have been confirmed in our calculations [see Figs. 4(c) and 4(d)]. Note that the mirror symmetry with respect to the point $\theta=0$ is not possessed by the spin-polarization component P_z, but is possessed by the total polarization P. A proof of the relation $P(-\theta)=P(\theta)$ is given in the Appendix. Thus when only the total polarization is concerned, we can restrict the value of θ to be in $[0,\pi/2]$. Furthermore, when a polarization plateau (intervals of full polarization) appears within the region $\theta\in(0,\pi/2)$, there should exist four polarization plateaus in the whole magnetic field orientation. This conclusion is reflected in Fig. 4(d). When a polarization plateau covers the angle $\theta=0$ or $\pi/2$, there are only two polarization plateaus in the whole region $[-\pi,\pi]$. The appearance of a polarization plateau, however, depends on the position of the Fermi energy relative to the band edges. In fact, when E is not within any (local) band gap, no polarization plateau appears. From Fig. 4(d) one can see that for $\mathbf{B}_{\text{in}}$ in parallel with or perpendicular to the wire axis, the spin polarization is small, especially in the case of $E=3.0$ meV. Therefore, for a proper Fermi energy, there exists several intervals of magnetic field angle within which an optimal spin polarization is achieved.

Finally, we examine how the Zeeman potential V_0 influences the spin polarization of the Rashba superlattice under different magnetic field angles. The typical results are shown in Fig. 5, where a relatively large Fermi energy is taken, $E=6$ meV. In all cases the degree of the spin polarization is nearly 100% as long as $V_0>E$ and a single polarization peak appears within the region $V_0<E$. The polarization direction and the position of the peaks, however, depend on the magnetic field angle θ. The results for $V_0<E$ can be explained as those in Fig. 3. The features for $V_0>E$ can be understood for a typical case $\theta=\pi/2$. In this case there exists no propagating mode in the superlattice region for spin-up incident electrons [see Fig. 2(c)]. For spin-down incident electrons, the transmission is either allowable (due to the presence of propagating modes) or shows a much slower decay (because the band edge is closer to E) in comparison with the spin-up incidence. Thus the spin polarization P_z is almost complete.

V. CONCLUSIONS

In conclusion, we have studied spin-dependent electron transport through a one-dimensional Rashba superlattice structure subject to a weak in-plane magnetic field $\mathbf{B}_{\text{in}}$. The

generated spin polarization and its direction of the considered system depend strongly on the orientation angle θ of $\mathbf{B}_{\text{in}}$ (relative to the transport direction). The total spin polarization is symmetric with respect to the angle $\theta=\pm\pi/2$ and $\theta=0$. For a given Fermi energy higher than the Zeeman potential, there may exist several intervals of θ within which an optimal spin polarization is achieved. For such θ values the Fermi energy falls into a local band gap of corresponding ideal Rashba superlattice where only two propagating (one right going and one left going) modes exist.

ACKNOWLEDGMENTS

This work was supported by the National Natural Science Foundation of China (Grant No. 10704013), the Specialized Research Fund for the Doctoral Program of Higher Education, the training fund of young teachers (Grant No. 893208), and the innovation fund of the Graduate School (Grant No. 703078) at the Dalian University of Technology.

APPENDIX: PROOF OF A SYMMETRY RELATION ON THE TOTAL POLARIZATION

The symmetry relation for the total polarization, $P(-\theta)=P(\theta)$, can be proved from the observation that the operation $\sigma_x R_x$ transforms the system with a magnetic field angle θ into that with the angle $-\theta$. This observation yields[17]

$$t_{\sigma\sigma'}(-\theta)=t'_{-\sigma,-\sigma'}(\theta), \tag{A1}$$

where $t'_{\sigma\sigma'}$ is the transmission amplitude for electrons with spin σ' incident from the right lead scattering into the spin σ state in the left lead. The symmetry associated with the operation $\sigma_y R_x T$ results in

$$t_{\uparrow\downarrow}(\theta)=t_{\downarrow\uparrow}(\theta)\equiv t_f(\theta). \tag{A2}$$

With Eqs. (A1) and (A2) we can write the scattering matrix for the system with the magnetic field angle θ as the form in Ref. 17,

$$S(\theta)=\begin{pmatrix} a\equiv r_{\uparrow\uparrow}(\theta) & b\equiv r_{\uparrow\downarrow}(\theta) & t_{\downarrow\downarrow}(-\theta) & t_f(-\theta) \\ c\equiv r_{\downarrow\uparrow}(\theta) & d\equiv r_{\downarrow\downarrow}(\theta) & t_f(-\theta) & t_{\uparrow\uparrow}(-\theta) \\ t_{\uparrow\uparrow}(\theta) & t_f(\theta) & r'_{\uparrow\uparrow}(\theta) & r'_{\uparrow\downarrow}(\theta) \\ t_f(\theta) & t_{\downarrow\downarrow}(\theta) & r'_{\downarrow\uparrow}(\theta) & r'_{\downarrow\downarrow}(\theta) \end{pmatrix}. \tag{A3}$$

Our expected result can be obtained from the orthogonality and normalization conditions of the first two columns (rows) of $S(\theta)$, which immediately result in $G(-\theta)=G(\theta)$. The combination of those conditions and the expressions of spin polarization [Eqs. (8) and (9)] leads to

$$[\tilde{P}(\theta)]^2=[|a|^2+|c|^2-|b|^2-|d|^2]^2+4(a^*b+c^*d)(ab^*+cd^*), \tag{A4}$$

$$[\tilde{P}(-\theta)]^2=[|a|^2+|b|^2-|c|^2-|d|^2]^2+4(a^*c+b^*d)(ac^*+bd^*), \tag{A5}$$

where $\tilde{P}(\theta)=P(\theta)G(\theta)/G_0$. The subtraction of Eq. (A5) from Eq. (A4) gives rise to $P(\theta)=P(-\theta)$.

*ya-zhang@hotmail.com
†fengzhai@dlut.edu.cn

[1] I. Žutić, J. Fabian, and S. D. Sarma, Rev. Mod. Phys. **76**, 323 (2004).
[2] E. I. Rashba, Fiz. Tverd. Tela (Leningrad) **2**, 1224 (1960) [Sov. Phys. Solid State **2**, 1109 (1960)]; Yu. A. Bychkov and E. I. Rashba, J. Phys. C **17**, 6039 (1984).
[3] G. F. Dresselhaus, Phys. Rev. **100**, 580 (1955).
[4] J. Nitta, T. Akazaki, H. Takayanagi, and T. Enoki, Phys. Rev. Lett. **78**, 1335 (1997); C.-M. Hu, J. Nitta, T. Akazaki, H. Takayanagai, J. Osaka, P. Pfeffer, and W. Zawadzki, Phys. Rev. B **60**, 7736 (1999).
[5] G. Engels, J. Lange, Th. Schäpers, and H. Lüth, Phys. Rev. B **55**, R1958 (1997).
[6] D. Grundler, Phys. Rev. Lett. **84**, 6074 (2000). In this work the Rashba spin splitting can be controlled under a constant carrier density by the application of both a back gate and a front gate to the quantum well.
[7] Y. Sato, T. Kita, S. Gozu, and S. Yamada, J. Appl. Phys. **89**, 8017 (2001).
[8] S. Datta and B. Das, Appl. Phys. Lett. **56**, 665 (1990).
[9] S. Bandyopadhyay and M. Cahay, Appl. Phys. Lett. **85**, 1814 (2004).
[10] C. Flindt, A. S. Sorensen, and K. Flensberg, Phys. Rev. Lett. **97**, 240501 (2006).
[11] A. Sarkar and T. K. Bhattacharyya, Appl. Phys. Lett. **90**, 173101 (2007).
[12] A. A. Kiselev and K. W. Kim, Appl. Phys. Lett. **78**, 775 (2001).
[13] J. I. Ohe, M. Yamamoto, T. Ohtsuki, and J. Nitta, Phys. Rev. B **72**, 041308(R) (2005).
[14] A. W. Cummings, R. Akis, and D. K. Ferry, Appl. Phys. Lett. **89**, 172115 (2006).
[15] F. Zhai and H. Q. Xu, Phys. Rev. B **76**, 035306 (2007).
[16] J.-F. Liu, Z.-C. Zhong, L. Chen, D. P. Li, C. Zhang, and Z. S. Ma, Phys. Rev. B **76**, 195304 (2007).
[17] F. Zhai and H. Q. Xu, Phys. Rev. Lett. **94**, 246601 (2005).
[18] F. Zhai and H. Q. Xu, Phys. Rev. B **72**, 085314 (2005).
[19] S. J. Gong and Z. Q. Yang, J. Appl. Phys. **102**, 033706 (2007).
[20] P. Středa and P. Šeba, Phys. Rev. Lett. **90**, 256601 (2003).
[21] Y. V. Pershin, J. A. Nesteroff, and V. Privman, Phys. Rev. B **69**, 121306(R) (2004).
[22] H. Tamura and T. Ando, Phys. Rev. B **44**, 1792 (1991).
[23] H. Q. Xu, Phys. Rev. B **50**, 8469 (1994); L. B. Zhang, F. Zhai, and H. Q. Xu, *ibid.* **74**, 195332 (2006).
[24] The $In_{0.75}Ga_{0.25}As$ 2DEG reported in Ref. 7 have both a much larger SOI strength and g factor than the GaAs 2DEG, and thus more suitable for the realization of the proposed device.
[25] S. J. Gong and Z. Q. Yang, J. Phys.: Condens. Matter **19**, 446209 (2007).